Preparation and Analysis of the Geometry Models used in the 1st AIAA Geometry and Mesh Generation Workshop

Nigel J. Taylor[1]
MBDA UK Ltd, Filton, Bristol BS34 7QW, UK

William T. Jones[2]
NASA Langley Research Center, Hampton, VA 23681-2199, USA

and

Mark Gammon[3]
ITI – International TechneGroup Ltd, Cambridge, CB24 4UQ, UK

The NASA High-Lift Common Research Model (HL-CRM) was the subject model chosen for the AIAA Geometry and Mesh Generation Workshop I (GMGW-1) and High-Lift Prediction Workshop III (HLPW-3). This paper describes how geometry models of the HL-CRM were prepared for use in the workshops and reviews the analysis of their construction that was provided to workshop participants. The refinements made to the HL-CRM geometry model immediately after GMGW-1 are also presented.

Nomenclature

BREP = Boundary REPresentation
CFD = Computational Fluid Dynamics
DPW = Drag Prediction Workshop
GMGW-1 = 1st AIAA Geometry and Mesh Generation Workshop
HL-CRM = High-Lift Common Research Model
HLPW-3 = 3rd AIAA High Lift Prediction Workshop
IGES = Initial Graphics Exchange Specification
MCAD = Mechanical Computer Aided Design
NASA = National Aeronautics and Space Administration
NURBS = Non-Uniform Rational B-Splines
OML = Outer Mold Lines
STEP = Standard for the Exchange of Product Model Data
WUSS = Wing Under Slat Surface

I. Introduction

In order to assess the readiness to meet challenges identified in the NASA CFD 2030 study,[1] the AIAA Meshing, Visualization and Computational Environments (MVCE) Technical Committee (TC) sponsored the first Geometry and Mesh Generation Workshop (GMGW-1) preceding the AIAA Aviation and Aeronautics Forum and Exposition (AIAA Aviation 2017). GMGW-1 was held in conjunction with the 3rd High Lift Prediction Workshop (HLPW-3). The primary focus of GMGW-1 was the NASA High-Lift Common Research Model wing-body (HL-CRM). This paper describes how geometry models of the HL-CRM were prepared for use in the workshops and reviews the analysis of their construction that was provided to workshop participants. The refinements made to the HL-CRM geometry model immediately after GMGW-1 are also presented.

[1] Capability Leader Aerodynamic Tools & Methods, AIAA Associate Fellow.
[2] Computer Engineer, Computational AeroSciences Branch, MS 128, AIAA Associate Fellow.
[3] Technical Director & CADfix Product Manager.

II. HL-CRM Geometry Model Preparation

The High Lift Common Research Model (HL-CRM) was developed to provide a relevant high lift geometry supporting collaborative high lift research.[2] The HL-CRM was derived from the High Speed variant of the Common Research Model (CRM) through the introduction of high lift devices. This geometry was delivered as a series of STEP files.

Individual STEP files were provided for the following components: the fuselage; main element with Wing Under Slat Surface (WUSS) and flap coves defined; nacelle and pylon; inboard and outboard slats; inboard and outboard flaps. High lift devices were supplied in their stowed positions and an additional STEP file was provided with coordinate reference frames for each deflection angle. For the purposes of the workshop, the additional file was used to position the components for a nominal landing configuration with slat and flap deflection angles of 30° and 37°, respectively. A final STEP file was provided with trimming planes defined for use in widening the spanwise gaps between flap components, see section D below. The geometry model, shown in Figure 1, represents a notional configuration for the purposes of HLPW-3, as there is no mounting hardware for the high lift devices (brackets, etc.).

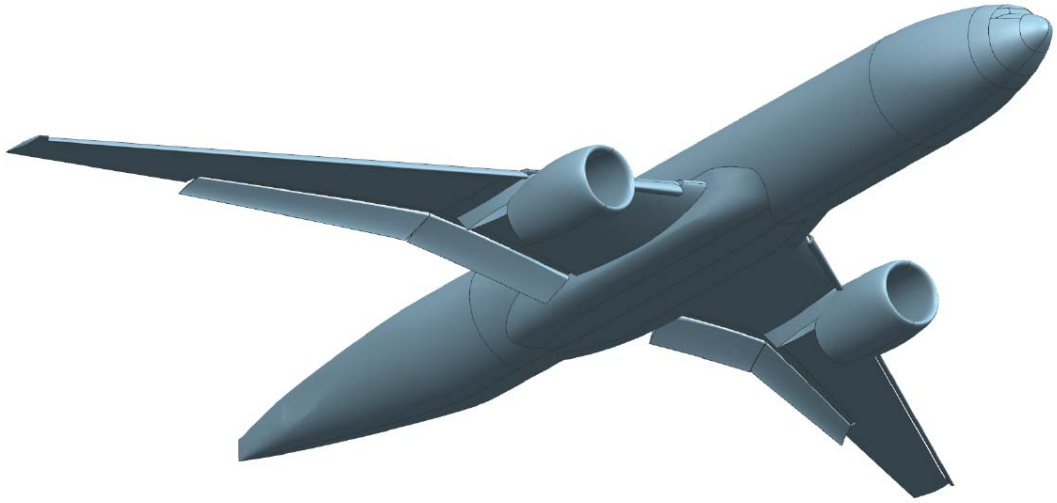

Figure 1. High Lift Common Research Model.

A. Nacelle and Pylon removal

For the purposes of HLPW-3, the nacelle and pylon were removed at the request of the organizing committee of that workshop. The nacelle and pylon were deemed unnecessary for HLPW-3, whose goal was to assess the numerical prediction capability of high lift systems through an initial mesh refinement study, and as such they were removed from the geometry model for simplification.

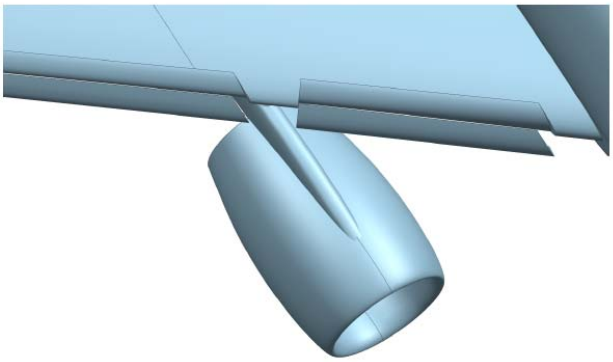

(a) Nacelle/Pylon prior to removal

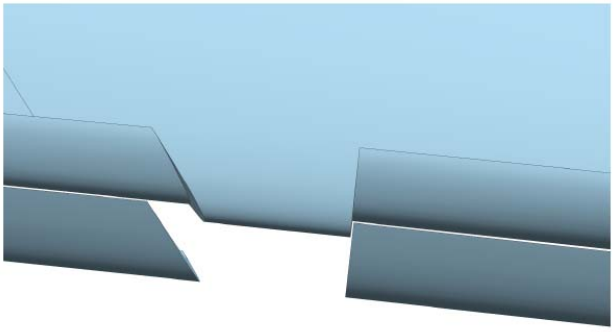

(b) WUSS protrusion with pylon removed

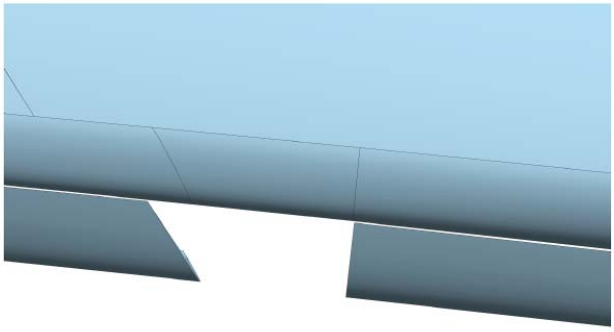

(c) WUSS protrusion removed

Figure 2. Removal of the WUSS protrusion.

B. Main Element

The removal of the pylon required a modification of the main element WUSS. The original geometry contained a protrusion that separated the WUSS into two segments. The protrusion was used to connect the pylon to the main element. With the pylon removed, it was the desire of the HLPW-3 committee to create a continuous WUSS through the removal of the protrusion. Removal of the protrusion would also be required for the creation of a single continuous slat element (described below, in section C). Protrusion removal was accomplished with a trimming operation that utilized the underlying continuous WUSS surface as a tool to remove the protrusion, as shown in Figure 2. The protrusion left by the pylon removal is seen in Figure 2(b) and the resulting continuous WUSS in Figure 2(c).

C. Slats

With the removal of the nacelle and pylon, it was the desire of the HLPW-3 committee to fill the spanwise gap between the inboard and outboard slats, thereby creating a single, uninterrupted slat element. A filler was produced as a loft between the end caps of the inboard and outboard slats and was forced to have G^1 continuity with its mating surfaces. This was done in favor of untrimming the inboard and outboard slat surfaces because doing so still left a very small gap that would have required further filling. Figure 3 shows the gap left by pylon removal in 3(a) and the resulting filler in 3(b).

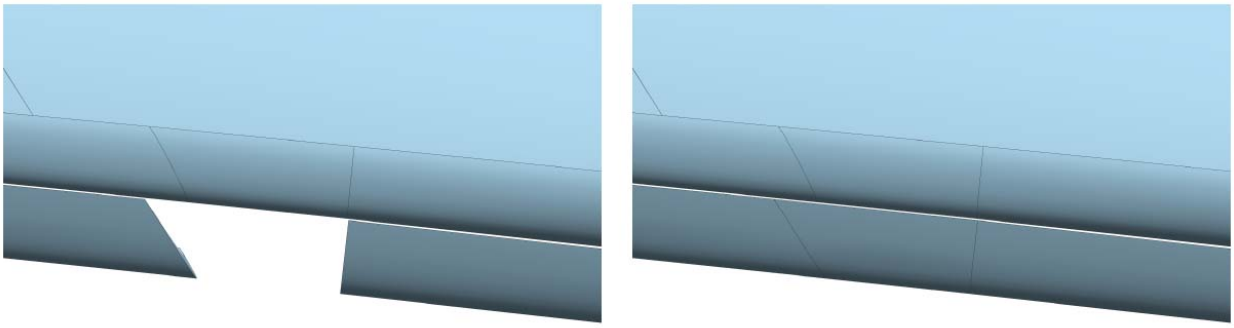

(a) Situation after pylon removal **(b) Single uninterrupted slat**

Figure 3. Treatment of the gap between the inboard and outboard slats created by removing the pylon.

D. Flaps

The HL-CRM employs two single-slotted flaps; delineated by the cranked trailing edge of the main wing and producing spanwise gaps, see Figure 4(a). When positioned in the representative landing configuration (37° deflection), the spanwise gap between inboard and outboard flaps (denoted midspan gap in Figure 4(a)) reduced to an extremely tight tolerance: the minimum gap between them is only 0.000918 inches, full-scale. As this tolerance is problematic for numerical mesh generation and is also likely to be unrealizable in physical models, the GMGW-1 and HLPW-3 committees decided to open the gap to 1.0 inch, full-scale.

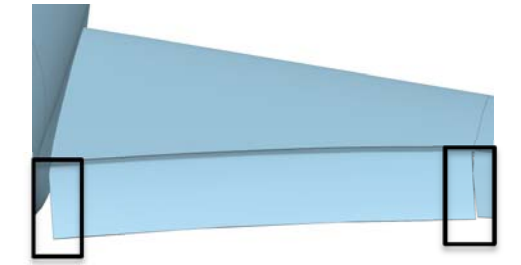

(a) Flap gap reference

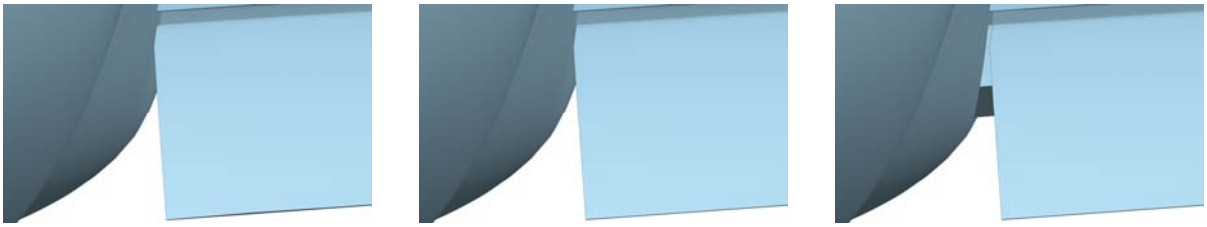

(b) As designed inboard gap **(c) Enlarged inboard gap** **(d) Partially sealed inboard gap**

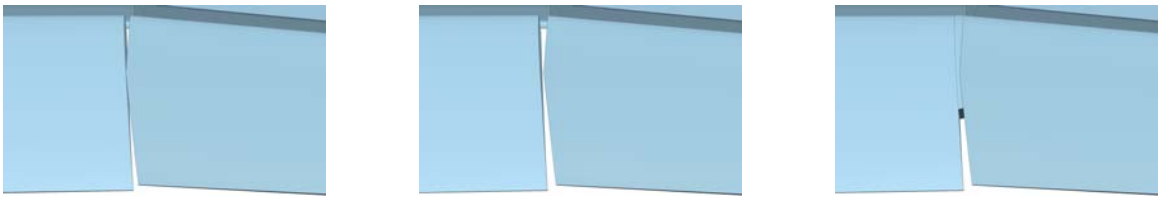

(e) As designed midspan gap **(c) Enlarged midspan gap** **(g) Partially sealed midspan gap**

Figure 4. Flap spanwise gap treatments .

The procedure to enlarge the gaps was similar to that of Reference [2]. An additional set of trimming planes was provided with the geometry in a STEP file. These planes were used to trim the elements in their stowed positions to

provide the desired 1-inch spanwise gaps at each end of the inboard and outboard flaps. The trimmed elements were then deflected to the 37° landing configuration setting. The resulting minimum gap after deflection is not exactly 1 inch, but is considerably larger than that of the untrimmed flaps (providing a minimum gap between the inboard and outboard flaps of 0.996 inches, full-scale).

In order to mimic a real aircraft, it was desired to produce a second model configuration by modelling a partial seal of the inboard and midspan flap gaps. This was accomplished by creating gap filler blocks on the 1-inch gap variant. These fillers are evident in Figure 4(d) and 4(g).

E. Fuselage

The provided fuselage was that of the high speed CRM. However this was delivered before the issues identified in Reference [3] were addressed. Therefore, as stated,[2] there remained abutment issues between some of the surfaces and associated topological issues, including those associated with the fuselage belly fairing, illustrated in Figure 5. These surfaces were derived from a structured CFD mesh. However, the discontinuities in the (wing- and fuselage-abutting) boundaries of the surface patches used to represent the belly fairing resulted in local overshoots and undershoots being generated at these corners. Three of these, highlighted in Figure 5 by red boxes, are detailed in Figure 6.

It was the decision of the GMGW-1 committee to leave the geometry as close to the as-delivered geometry as possible so as to identify real world issues. However, it was also recognized that inconsistencies in the model (holes, gaps, and overlaps) should be repaired prior to dissemination to the workshop participants so as to create a consistently complete representation. Therefore, an attempt was made to address the abutment issues illustrated in Figure 6 prior to making the geometry models available to workshop participants.

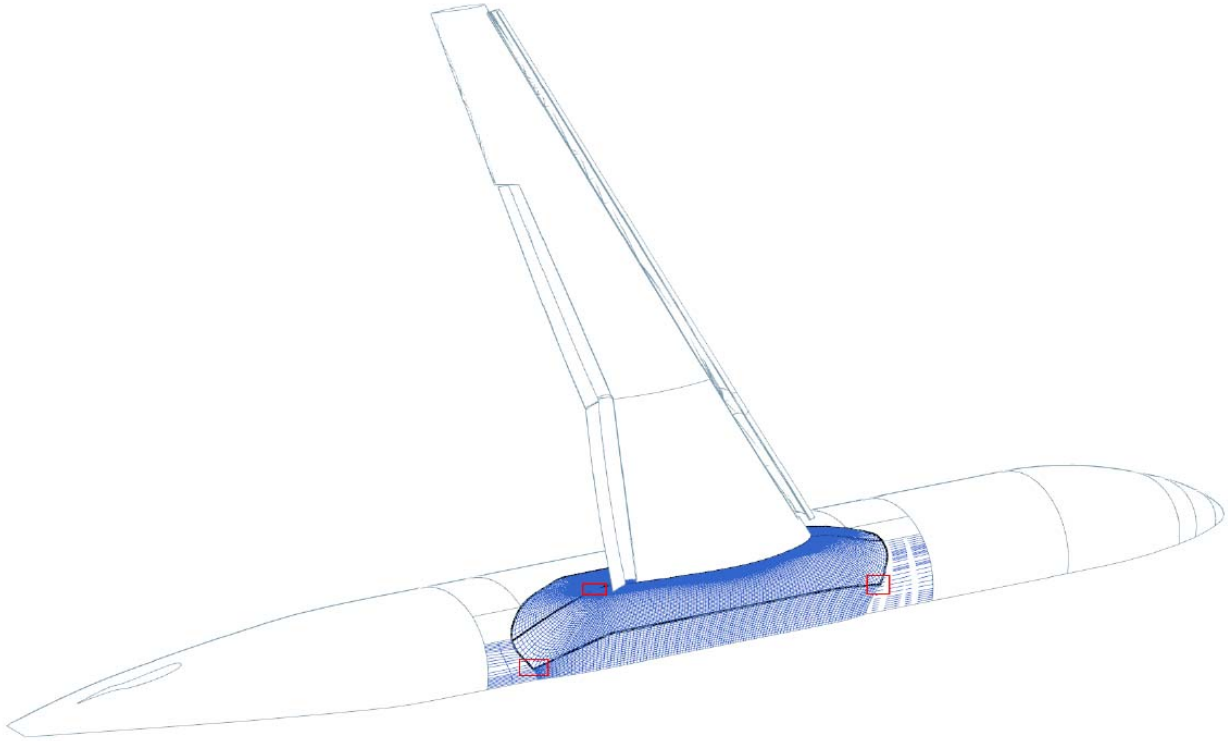

Figure 5. Some of the problem areas on the original Fuselage Belly Fairing surfaces.

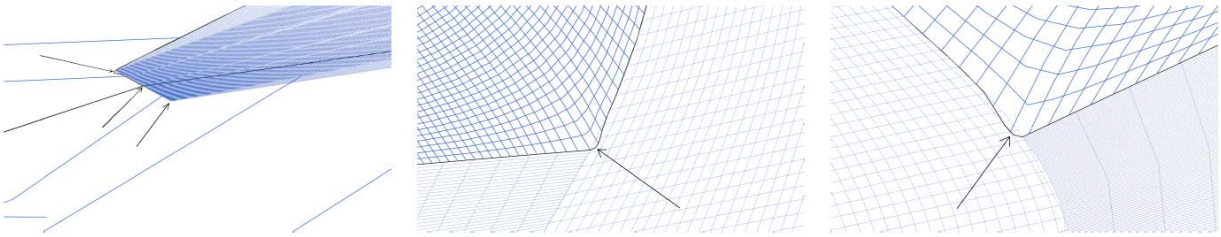

(a) Wing trailing edge intersection **(b) Forward lower corner** **(c) Aft lower corner**

Figure 6. Details of the Fuselage Belly Fairing highlighted in Figure 5.

The method used to repair the fuselage belly fairing, using GridTool,[4] was as follows. First the original Non-Uniform Rational B-Spline (NURBS) surface was evaluated at the knots to recover the original interpolating structured surface grid. This surface grid was then broken into six distinct components at each boundary discontinuity. Six new NURBS surfaces were then interpolated to each of the distinct surface component grids. An additional ruled surface was created to fill the hole created by the wing intersection. Those seven surfaces then served as a basis for the creation of a new topology that defined the fairing using four faces.

The surfaces adhering to this new topology were created using the Quilting technique in the NX Computer Aided Design system, version 10.0. This technique was used to combine several surfaces into one by creating a single NURBS surface that approximates a four-sided region lying near several existing surfaces. The system projected sample points from a driver surface along the driver surface normal vectors (or a user specified vector) onto the target surfaces (those being approximated). The projected points were then used to construct an approximating NURBS surface. The driver points were adapted to satisfy a modeling error tolerance, which in this case was 0.001 inches. In order to minimize errors in the approximation, the topology of the driver surfaces, rendered gray in Figure 7, was selected.

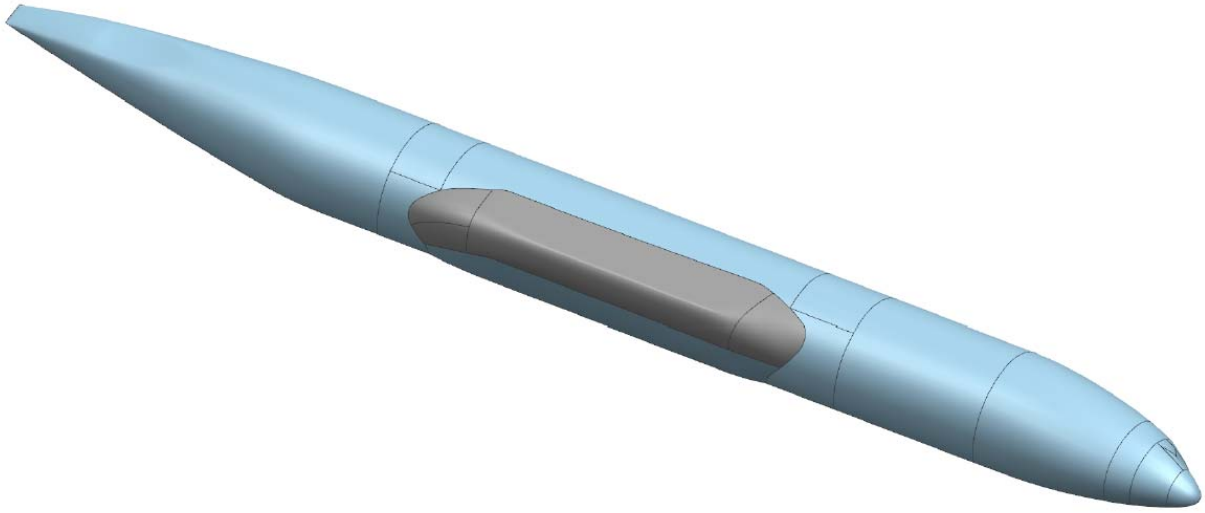

Figure 7. Modified Fuselage Belly Fairing topology.

F. Dissemination

It was the decision of both the GMGW-1 and HLPW-3 organizing committees to release the geometry model in a variety of native and standard formats. The geometry assembly and modifications were made in Siemens NX, version 10.0. As such, the native NX part file was the primary distribution medium. Also, as Parasolid is the underlying geometry kernel of NX, a Parasolid XT transmit file was provided. However, it was recognized that participants may work in other systems and therefore the geometry was provided in both IGES and STEP formats. The Parasolid XT, IGES, and STEP files were exported directly from NX. Finally, as the NASA model designers imported the Parasolid XT files into Creo for additional design of the wind tunnel model (brackets, internal structure, instrumentation, etc.), it was the decision of the GMGW-1 committee to provide a native Creo file of the model. Note that the Creo file was

created by simply importing the Parasolid XT version of the geometry and saving as a Creo part file. All formats of the geometry were provided for both the gapped flap and the partially sealed flap configurations.

The generated Parasolid XT and STEP files were imported into a variety of software packages to test for validity prior to dissemination. The Parasolid XT files were shown to import successfully into: Creo 2.0; SolidWorks 2014; Ansys Workbench 16; and CADfix 10 (where the CADfix "Repair" operation reported nothing needed). Likewise the STEP files were successfully imported into: Creo 2.0; SolidWorks 2014; AnsysWorkbench16; CADfix 10 (and again the CADfix "Repair" operation reported nothing needed); and FreeCAD, an OpenCASCADE-based MCAD system.

III. Pre-Workshop Analysis

A. Scope and Objectives

Prior to the Workshop, the authors subjected several of the supplied models to a simple analysis. The objective of this was to identify those aspects of their construction that might have a bearing on the subsequent requirements for mesh generation. No formal process or checklist was adopted; instead, we simply followed our noses, recognizing that a prerequisite of many mesh generation processes is a topologically watertight Boundary REPresentation (BREP) of the airframe. No direct comparisons of the Outer Mold Lines (OML) contained in the models were made and no attempt was made to assess the physical significance of any differences observed. Consequently, the results are not considered to be comprehensive or definitive. However, despite these limitations, several issues that are commonly encountered in preparing geometry models for mesh generation were identified. A brief summary of the principal findings is provided below. However, it is helpful first to explain what is meant by a “topologically watertight BREP.”

B. Topologically Watertight BREP

The prevalent way in which solids are currently modeled in engineering applications is via the judicious use of BREPs. These are formed almost exclusively by intersecting two-dimensionally parametric surface patches, as required; the resulting (trimmed) regions of each surface patch between the intersections forming a component of the BREP, as illustrated in Figure 8. This shows a small region of a BREP formed by two intersecting surface patches, S1 and S2. Figure 8(a) identifies the key underlying properties of both surface patches: their vertices (only the trimmed vertices are labelled), their edges, their underlying (two-dimensional) parameterization (represented by the blue mesh) and the curve defining the intersection between them (E1). For simplicity, Figure 8(b) identifies the contributions made by these surface patches to the overall BREP of a cube. Note that, in order to maintain the integrity of the trimmed surface patch definitions, it is necessary to maintain the untrimmed portions of the underlying surface patches as part of the BREP model (in general, their removal would modify the shape of the trimmed patches).

The following features of Figure 8 are particularly noteworthy:

(i) Each surface patch – trimmed or untrimmed – is bounded by a series of edges connecting vertices. These vertices must be connected in an order that allows the windward side of each surface patch to be identified correctly, meaning that each edge must be defined in a specific direction and connected in sequence. (Conventionally, the required direction is counterclockwise when viewed from the outside.) The vertices shared by adjacent trimmed surface patches – i.e., those delineating the exposed ends of intersection curves – must therefore be connected in opposite directions when used to define the trimmed surface patches they bound.

(ii) While the underlying untrimmed surface patches are parametric, their intersections are not: in general, they are evaluated on a point-by-point basis, in each case the result only being accurate to a predefined tolerance. Consequently, intersection curves do not necessarily lie precisely on the trimmed surface patches they are considered to bound. Moreover, it follows that, while the edges bounding an untrimmed surface patch will follow a closed loop, those associated with a trimmed surface patch might not (vertices at the “intersecting” ends of two intersection curves may not be perfectly coincident).

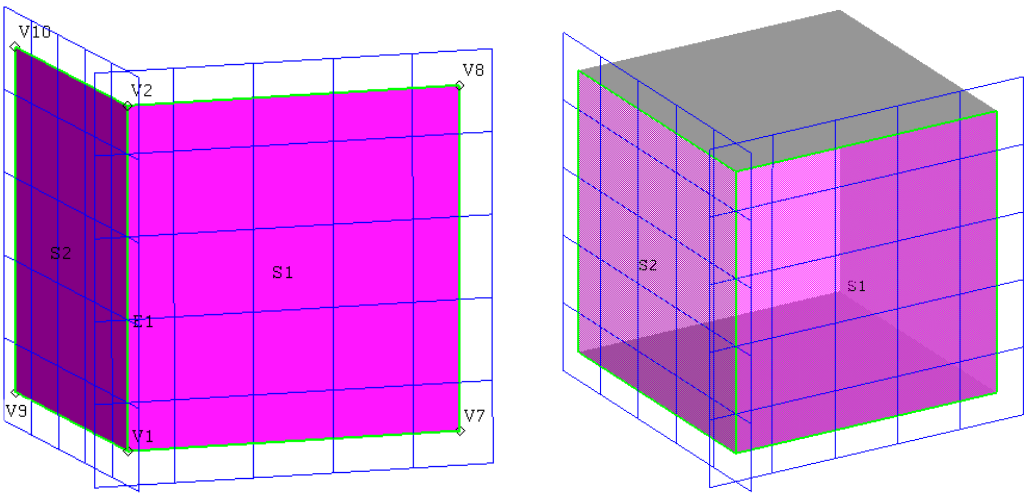

(a) Underlying parametric surfaces **(b) Their contributions to a simple BREP**

Figure 8. Simplified illustration of the way in which parametric surfaces are used to form BREPs

Unfortunately, there is no known way of completely avoiding these "leaks" when using the form of BREP illustrated in Figure 8. Thus, the OML defined in this way will not, in general, be perfectly watertight. To build a measure of robustness against the inevitable leakage, contemporary mesh generation tools tend to require merely that the OML are topologically watertight – that is, that only the bounding curves of the trimmed surface patches need be watertight - and even then only to a permissible tolerance. (Any local leakage that may occur between adjacent surface patches is simply meshed over on the basis that the attendant effect on the local OML is very small indeed – usually appreciably smaller than the local surface mesh cells and well within manufacturing tolerances. This is in keeping with the fact that the juncture was not unambiguously defined in the first place.)

C. NX Model

To provide a baseline against which the other supplied models would be judged, the first of the supplied models analyzed was the NX Model. This consists of 66 surfaces, 12 of which are analytical (planes or cylinders). The latter, highlighted in blue in Figure 9, represent: the planes used to trim the flaps in order to introduce the 1-inch gaps; a symmetry plane to seal the half-span model; and other construction entities used to assemble and examine the model in NX. While the trimming planes were included in the original collection of STEP files, the remaining analytical surfaces were introduced following the import of these files into NX in the process of sewing up the surface model into a complete BREP.

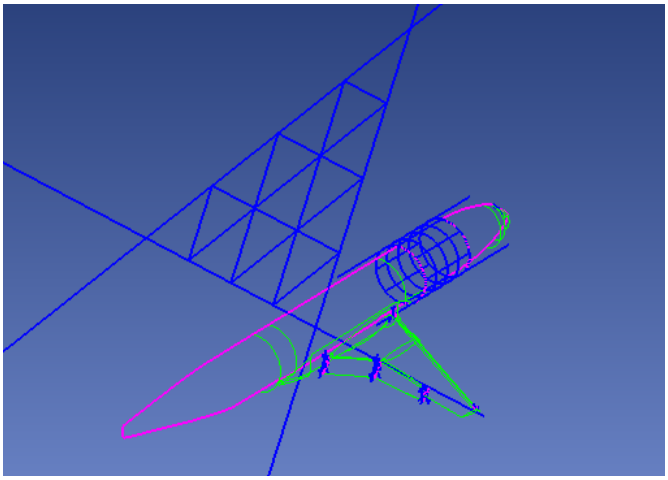

Figure 9. Bounding Curves in the NX Model: blue items are associated with Analytical Surfaces (Cylinders or Planes)

Another noteworthy aspect of the NX Model construction is that the underlying parameterization of several of its surface patches were unexpectedly dense and/or non-uniform. Localized undulations in surface curvature were also observed in several places. While some of these features may have been inherited from the original STEP files, this is not always the case. Moreover, the degree of the NURBS used to form some of the surfaces generated specifically for GMGW-1 was not consistent – for instance degree 5 NURBS are present on the WUSS, cf. degree 3 NURBS predominate elsewhere. Some examples of these features are illustrated in Figures 10 – 13, below.

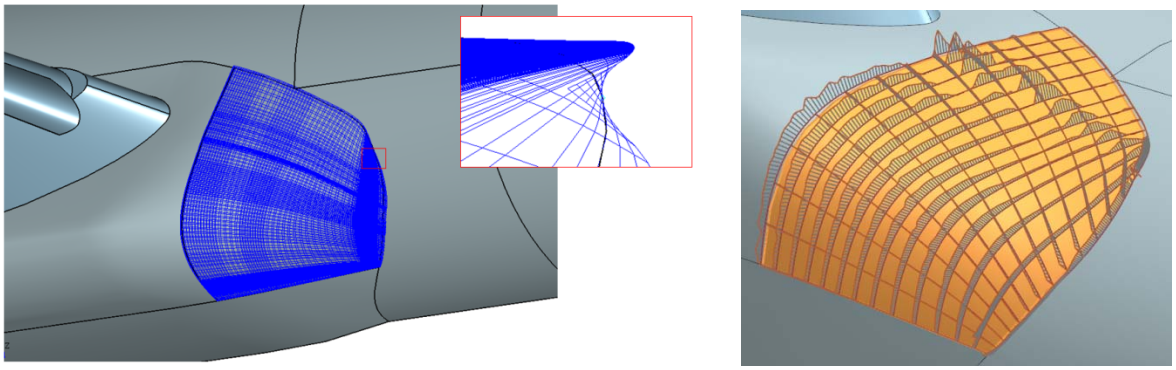

(a) Underlying surface construction details (Selection of isoparametric curves)

(b) Local surface curvature

Figure 10. Forward Region of the Belly Fairing in the NX Model.
(Additional note: The size of the fold in the highlighted surface patch is ~0.1in, full-scale)

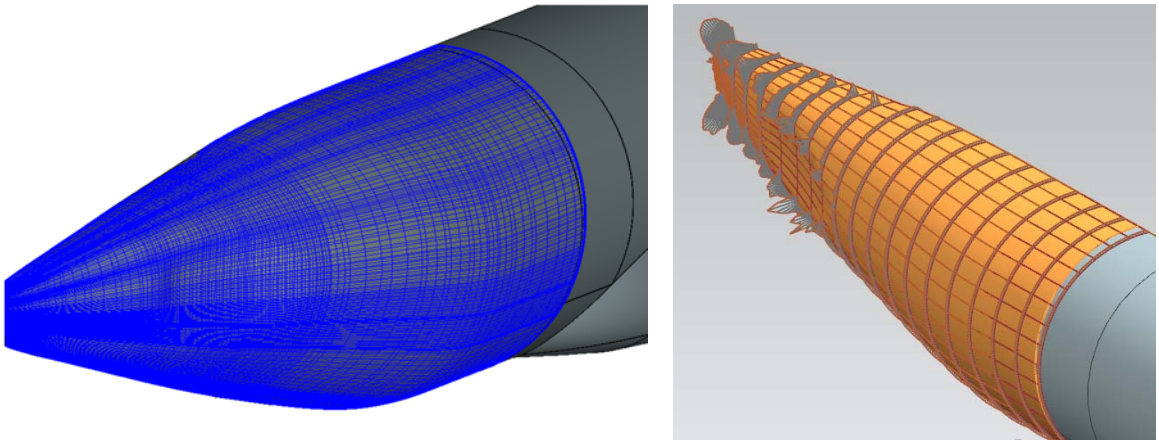

(a) Underlying surface construction details (Selection of isoparametric curves)

(b) Local surface curvature

Figure 11. Rear Fuselage in the NX Model.

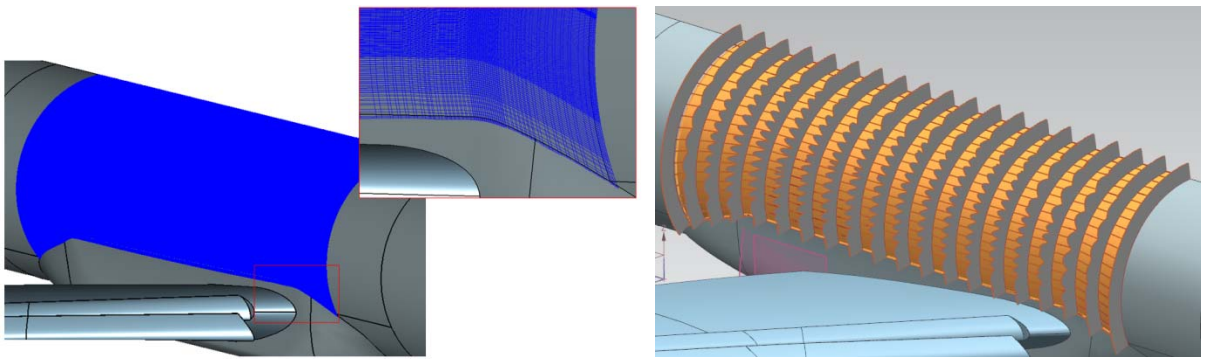

(a) Underlying surface construction details (Selection of isoparametric curves)

(b) Local surface curvature

Figure 12. Central Fuselage in the NX Model.
(Additional note: The number of control points used to define this patch is $O(10^6)$)

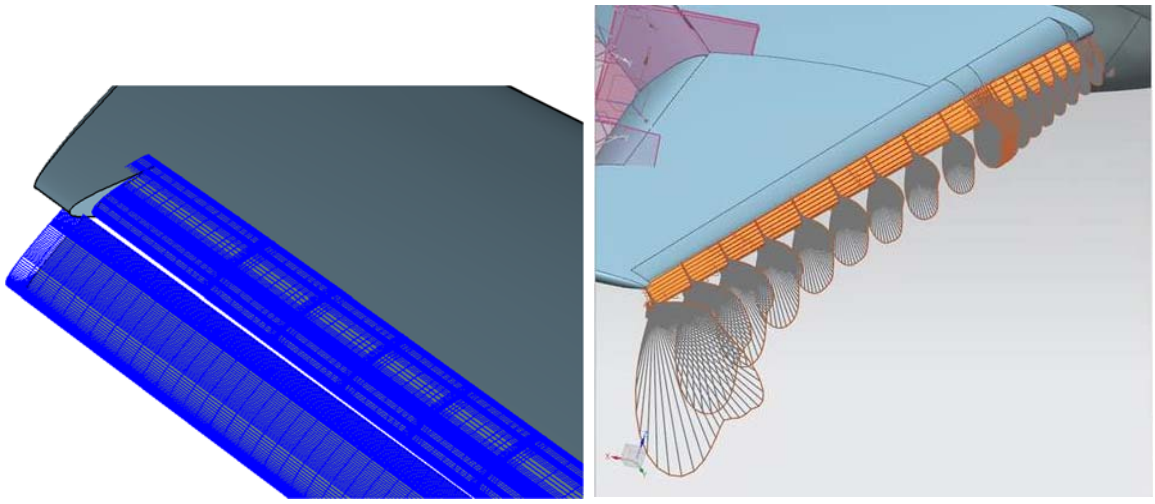

(a) Underlying surface construction details (Selection of isoparametric curves)

(b) Local surface curvature

Figure 13. Slat and WUSS in the NX Model.
(Additional note: The WUSS is defined as an offset surface – and as such is not currently amenable to surface curvature analysis in NX.)

Subsequent to the independent analysis of Dannenhoffer,[5] the construction of the trailing-edge flap coving was inspected. The results, illustrated in Figure 14, identified that varying degrees of spanwise waviness were present in the OML along the full extent of both flap segments.

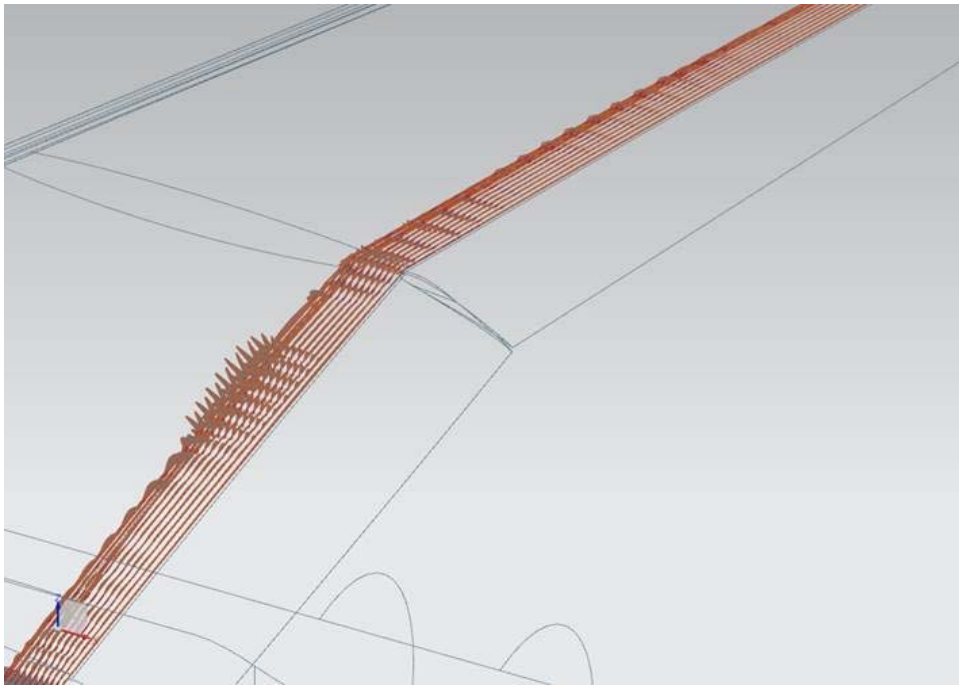

Figure 14. Spanwise waviness in the trailing-edge flap coving in the NX Model.

It should be stressed that the irregularity and/or inconsistency of these features were not introduced into the NX Model intentionally – and serve to illustrate the difficulties that can be faced by even the most experienced practitioners, intimately familiar with the requirements of mesh generation, in generating geometry models for use with CFD.

D. STEP file (hl-crm-gapped-flaps.stp.gz)

The geometry model provided in the STEP file retained the principal topological features of the NX Model – it consisted of 66 surface patches and possessed the same overall number of edges (334). However (i) the maximum geometric leakage between the bounding curves was ~0.00147in. (0.04mm) – i.e., slightly outside the specified NX modelling tolerance (0.001in.); (ii) the WUSS was approximated using a degree 3 NURBS and was not represented using an off-set surface.

Figure 15 contains a sample of the results of an independent analysis, conducted by Dannenhoffer.[5] Simplified contours that illustrate the distributions of nondimensional measures of the product of the principal curvatures on each surface patch are evaluated throughout the trimmed region of each surface on the OML Many of the features described in Section C, above (and a few more), are evident.

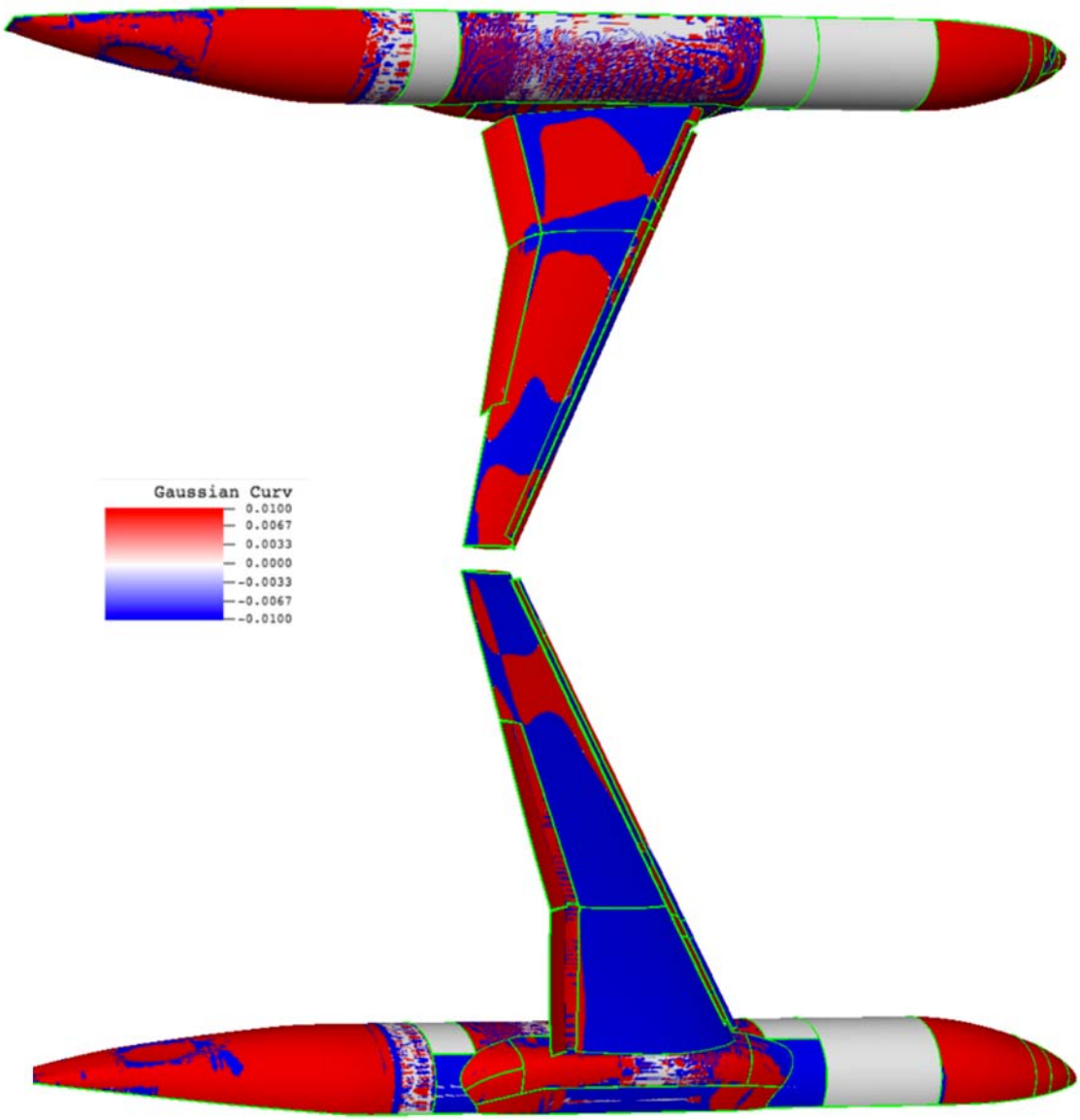

Figure 15. OML Gaussian Curvature Analysis of the HL-CRM OML.[5]
(Top: View from above; Bottom: View from below)

E. IGES file (hl-crm-gapped-flaps.igs.gz)

The topology of the geometry model provided in the IGES file differed from that of the NX Model in several respects. For instance: (i) 10 of the surfaces used to define the slat and belly fairing - see Figure 16 - are not trimmed; (ii) those trimming curves that are included are often more fragmented than those present in the NX Model. Unfortunately, NX v10 does not support the export of IGES Entities of Type 141 or 143. Consequently, this places a greater onus on the downstream software (or user) to recover lost connectivity. Interestingly, unlike the situation with the STEP file, the geometry model provided in IGES format represents the WUSS as an order 5 offset surface.

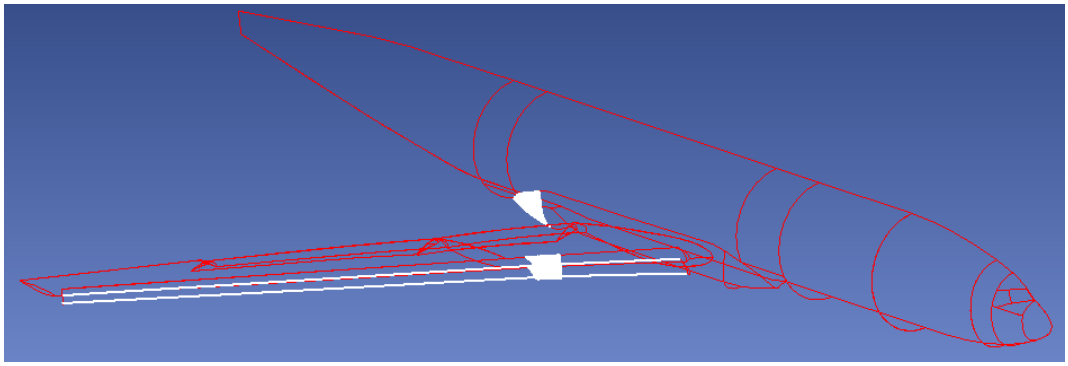

Figure 16. Bounding Curves in the geometry model provided in the IGES file. Those associated with untrimmed surfaces are colored white.

F. CATIA model

In response to an informal request from a GMGW-1 participant for a geometry model to be supplied for use in CATIA, attempts were made to import the STEP file into CATIA v5. (CATIA models cannot be generated directly using NX v10.) This proved unexpectedly problematic. After some effort (the precise details of which were not recorded at the time), it became apparent that one source of difficulty was that several of the surface patches - particularly those used to define the central fuselage - were being split into a very large number of very small fragments on import – see Figure 17. (Another was that importing the fuselage belly fairing surfaces proved problematic; this is also evident in Figure 17.) Following inquiry with the vendor, it transpired that this was happening because of a strict requirement of surfaces in CATIA: that they possess C2 continuity everywhere. Thus, in performing the series of checks to which all models are subjected to during import into CATIA, localized variations in surface curvature were encountered (evident in Figure 12). As a result, noncompliant surfaces were partitioned along isoparametric lines until each surface so-created was C2 continuous throughout. Resolving this issue would have required noncompliant surfaces to be smoothed. However, since this was contrary to the principles adopted in generating the models for use in GMGW-1, no CATIA model of the HL-CRM was made generally available to workshop participants.

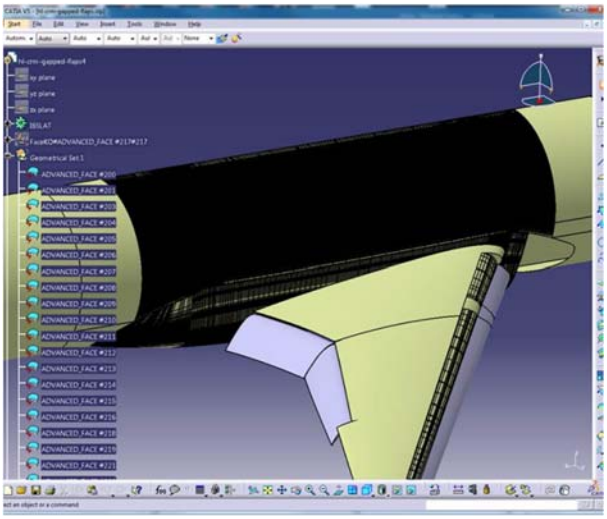

Figure 17. Representation of the central fuselage region in CATIA v5. (Black lines indicate trimmed surface boundaries)

IV. Addressing Workshop Findings

The topology used for the quilting operation in section II, subsection E, was selected in an effort to minimize the error in the approximating surfaces. This was subsequently found to be problematic upon detailed analysis and mesh generation by GMGW-1 participants. As a result, the method was altered by first extending, through extrapolation, the outer boundaries of the seven basis surfaces that had been interpolated to the distinct surface grid components using NX. A series of 100 longitudinal sections were created to include the surface extensions. These were then used, along with the collective bounding waterlines, to create a new single surface loft for the wing/body fairing. That surface was then exported via IGES and loaded into GridTool.[4] The seven extended basis surfaces were also loaded into GridTool via IGES. A structured grid of the relofted fairing surface was created in GridTool by evaluating the surface at the NURBS knots. The resulting structured grid was then projected onto the extended basis surfaces via GridTool and a final NURBS surface was interpolated to the projected surface grid. The projected fairing surface was then exported to NX via IGES. Upon loading into NX, the projected fairing surface was trimmed by edges of the neighboring fuselage surfaces to reveal the final fairing shape. This resulted in an improved surface parameterization topology with minimal loss of accuracy. The result is shown in Figure 18. Like the preceding repair, the new fairing surface results in no predefined hole for the wing intersection. This added benefit eliminates the potential for problems like those seen in Figure 6(a).

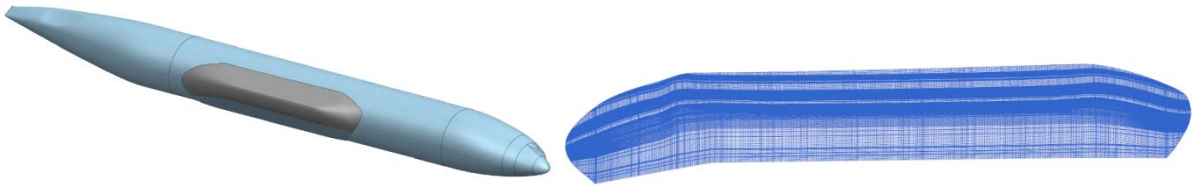

(a) Surface Topology

(b) Underlying Trimmed surface construction (Selection of isoparametric curves)

Figure 18. New Fuselage Belly Fairing topology

The opportunity was also taken to simplify the construction of the fuselage surfaces above the wing: the circular cylinder surfaces were replaced with a simple loft of the opposing circular cross sections. This repair is also visible in the topology of Figure 18 (cf. Figure 7). An updated suite of geometry models has been posted on the HLPW-3 website.

V. Closing Remarks

While the construction of the HL-CRM is appreciably simpler than the geometry models encountered in many industrial contexts, the fact that the models are open and can be shared has allowed several of the problems that are commonly encountered in preparing for CFD mesh generation to be illustrated and described. These problems can be grouped under two headings:

(i) Interoperability: No two variants of the models supplied to workshop participants were identical. Model translation (from one format or operating platform to another) can be an issue for upstream and downstream processes.

(ii) Inadvertent introduction of small geometric features: This can be a problem even for experienced practitioners who are well-versed in the requirements for mesh generation and CFD.

It should be stressed that all geometric modelling is subject to tolerancing and that no attempt has yet been made to assess the potential aerodynamic significance of the various irregularities described herein. However, at the time of writing, subject to the prescription (and attainment) of suitable geometric tolerances, it appears that the types of irregularity described herein are likely to present more profound challenges for the development of robust, automated, end-to-end CFD simulation processes than they are to have discernable implications for the outputs of CFD computations.

References

[1]Slotnick, J., Khodadoust, A., Alonso, J., Darmofal, D., Gropp, W., Lurie, E., and Mavriplis, D., “CFD Vision 2030 Study: A Path to Revolutionary Computational Aerosciences," NASA CR-2014-218178, 2014.

[2]Lacy, D. S. and Sclafani, A. J., “Development of the High Lift Common Research Model (HL-CRM): A Representative High Lift Configuration for Transonic Transports," *54th AIAA Aerospace Sciences Meeting*, San Diego, CA, AIAA 2016-0308, January 2016.

[3]Taylor, N. J., Gammon, M., and Vassberg, J. C., “The NASA Common Research Model: A Geometry-Handling Perspective," *46th AIAA Fluid Dynamics Conference, AIAA Aviation Forum*, Washington, D.C., AIAA 2016-3486, June 2016.

[4]Samareh-Abolhassani, J., “GridTool: A Surface Modeling and Grid Generation Tool," *Proceedings of the Workshop on Surface Modeling, Grid Generation, and Related Issues in CFD Solutions*, NASA CP-3291, NASA Lewis Research Center, Cleveland, OH, 9-11 May 1995, p. 11.

[5]Dannenhoffer, J, D, *private communication*, 15 November 2017.